

Bifurcation analysis points towards the source of beta neuronal oscillations in Parkinson's disease

Dr Alejo J Nevado-Holgado, Dr John R. Terry, Dr Rafal Bogacz

Abstract—Parkinson disease is the second most common neurodegenerative disorder after Alzheimer, affecting 0.16% of the population in the USA¹. This disease is most common in the elderly, what makes it a prominent health problem in developed countries, where the elder population is expected to importantly increase in the future. The mechanism generating the disease is the death of dopaminergic neurons in the substantia nigra pars compacta (SNc), a small brain region from the brain stem. These neurons release the neurotransmitter dopamine to the basal ganglia, a large and complex brain structure implicated in motor control and reinforcement learning. Once SNc neurons have died, the basal ganglia starts showing prominent features of malfunction, and the characteristics symptoms of Parkinson's disease began to be observed in the patient (i.e. general difficulty or inability to execute motor movements and limb tremor, among others). Modern theory of Parkinson's disease focuses on the abnormal brain activity oscillations observed in the basal ganglia, which are consistently observed in parkinsonian patients and correlate with their symptoms. This paper develops a mathematical model of the basal ganglia, which reproduces the experimentally recorded neuronal activity of this brain structure in health and disease. Studying this model numerical and analytically, we draw conclusion on how and where these oscillations are generated within the brain. If the conclusions of this mathematical model are further confirmed experimentally, we think they pave the way towards controlling such oscillations pharmacologically or through electrode stimulation in the future.

I. INTRODUCTION

Parkinson's disease is one of the most common neurodegenerative disorders, but the mechanisms giving rise to the disease are not yet well understood. It is known that the death of dopamine producing (i.e. dopaminergic) neurons in the substantial nigra pars compacta (SNc, a brain stem nucleus) closely correlates with the onset and advance of the disease [1], [2], [3], [4], [5], [6], [7], [8], [9], [10]. These dopaminergic cells project in the healthy brain to all major nuclei of the basal ganglia, a complex network of nuclei with important implications in motor control and decision making [11], [12], [13], [14], [15], [8], [9] (see figure 1).

Department of Experimental Psychology, University of Cambridge, Cambridge, UK ajn39@cam.ac.uk

Sheffield Institute for Translational Neuroscience, University of Sheffield, Sheffield, UK j.r.terry@sheffield.ac.uk

Department of Computer Science, University of Bristol, Bristol, UK R.Bogacz@bristol.ac.uk

Dr Alejo J Nevado-Holgado was funded by Caja Madrid Foundation, Madrid, Spain consultasfundacion@cajamadrid.es

¹data from National Institute of Neurological Disorders and Stroke, USA.

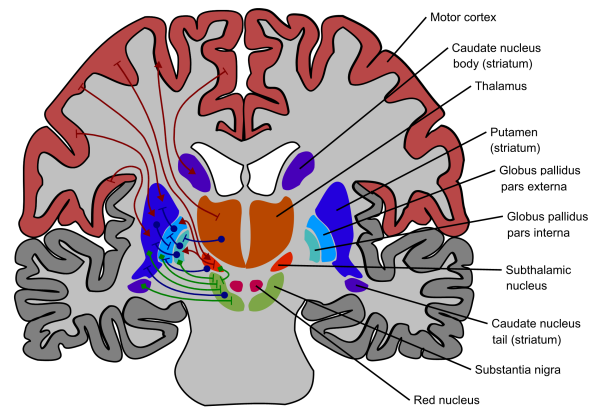


Figure 1. Brain structures implicated in Parkinson's disease - cortico basal ganglia loop. The left side of the diagram shows the connectivity of the basal ganglia network, while the right side indicates the names of each brain structure. Brain structures which project excitatory axons are filled with colours from the red spectrum, inhibitory structures with colours from the blue spectrum and modulatory structures with green colours. Arrows represent known axon projections, where the colour and the arrow head shape indicate the nature of the implicated axons. Red with triangular head represent excitatory fibers, blue with circular head represents inhibitory and green with rhomboidal head, modulatory.

In the parkinsonian state, the absence of the dopaminergic connections projecting to basal ganglia nuclei, produces an imbalance in both the mean neuronal activity of these nuclei and its oscillations [16], [17], [18], [7]. This double-sided imbalance seems to perturb in some unknown manner the correct functioning of the basal ganglia, which is no longer able to select and execute the voluntary movements that are coded in the motor cortex [19], [8]. Several decades ago, a conceptual model was proposed to explain the relationship between the mentioned physiological abnormalities of the basal ganglia and the observed external symptoms of Parkinson's disease [20], [3], [21], [7], [22]. This model focused on explaining the imbalances in mean firing rates (i.e. the measure of neuronal brain activity), and was able to explain the early experimental observation made on parkinsonian patients and animals.

More recent results have challenged the full validity of this model, and recent studies are rather focusing on the role of firing rate oscillations, whose frequency spectrum consistently changes from the healthy to the diseased condition [23], [16], [17], [18]. This frequency spectrum shows

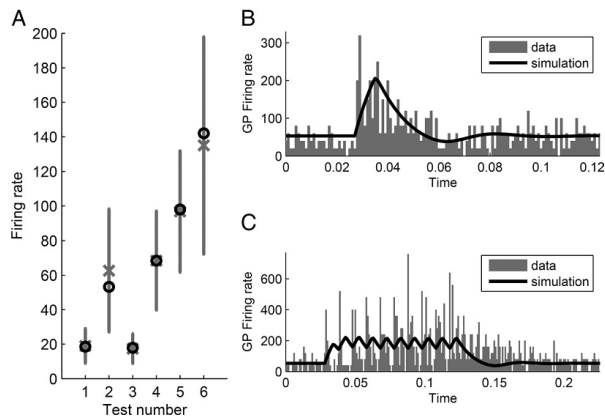


Figure 2. Comparison of model behaviour with experimental data obtained from healthy monkeys. Vertical axes indicate firing rate in units of spikes per second. A: Measures of STN’s and GPe’s mean firing rate in different experimental situations. Grey crosses show the mean experimental values and vertical lines indicate standard deviations. This is compared with the mean firing rate of the model in the same situations indicated by black circles. The numbers under the x -axis correspond to: (1) natural average STN; (2) natural average GPe; (3) GPe while $STN \rightarrow GPe$ transmission is blocked; (4) GPe while $STN \rightarrow GPe$, $GPe \rightarrow GPe$ and $Str \rightarrow GPe$ transmission are blocked; (5) GPe while $GPe \rightarrow STN$ is blocked; (6) GPe while $GPe \rightarrow GPe$ and $Str \rightarrow GPe$ are blocked. B: GPe firing rate after single stimulation of STN [29]. Grey bars show experimental data and black curve corresponds to the results of simulation. C: GPe firing rate after burst high frequency stimulation of STN [29].

three distinct frequency bands (theta 4-7Hz, beta 12-30Hz and gamma 30-100Hz) and their relative prominence changes with the onset of the disease. Results suggest that beta band blocks the execution of voluntary movements (or at least it consistently co-occurs with motor suppression), while gamma band seems to be present when voluntary movements are executed. Conversely, theta band may be related with the symptom of limb tremor, given the similarity on the frequency of oscillations [24], [25], [26], [27], [28]. Given its alleged close relationship with motor impairment, it would be important to know how and/or where beta oscillations are generated, as controlling or suppressing such oscillations may influence motor impairment.

II. METHODS

A. Mathematical model

The STN-GPe network is a mutually coupled system, where STN neurons project excitatory glutamergic axons to the GPe [30], whilst GPe neurons project inhibitory GABAergic axons to the STN and to other neurons within GPe [31]. Additionally, these two nuclei receive inputs from cortex and striatum respectively [32]. To characterise the firing rate of neural populations in STN and GPe we use the well described firing rate model [33], [34]. Using the equation of the mean firing rate model to model STN and GPe populations, we obtain the following set of equations describing our model:

Table I
VALUES FOR FIXED PARAMETERS.

Parameter	Value	source
Δt_{SG}	6 ms	[29]
Δt_{GS}	6 ms	Extrapolation to monkeys based on [37]
Δt_{GG}	4 ms	Based on proximity between cells
τ_S	6 ms	[38], [39], [40]
τ_G	14 ms	[41]
Ctx	27 spk/s	[42]
Str	2 spk/s	[43]
M_S	300 spk/s	[44]
B_S	17 spk/s	[44]
M_G	400 spk/s	[29], [32]
B_G	75 spk/s	[45], [32]

This table shows the model parameters whose values were directly established from the experimental literature. For each parameter, the used value and the literature source are shown.

$$\begin{cases} \tau_S \dot{STN} = -STN(t) + F_S(-w_{GS}GP(t - \Delta t_{GS}) + w_{CS}Ctx) \\ \tau_G \dot{GP} = -GP(t) + \\ F_G(w_{SG}STN(t - \Delta t_{SG}) - w_{GG}GP(t - \Delta t_{GG}) - w_{XG}Str) \end{cases} \quad (1)$$

where STN and GP are, respectively, the firing rates of the STN and GPe neural populations. Ctx and Str are the constant inputs from cortex and striatum, respectively. Although beta oscillations have been reported in the cortex and the striatum [35], [36], we wish to explore whether the STN-GPe network could generate beta oscillations independently of an external oscillatory drive. Consequently, we do not explicitly model corticostriatal interactions and consider these inputs to be constant, implying that any oscillatory phenomena appearing in our model will be exclusively due to the STN-GPe network. τ_S and τ_G are the time constants for STN and GPe populations, respectively. $F_S(\cdot)$ and $F_G(\cdot)$ are the input-output relationships for STN and GPe populations. w_{AB} are the weights of the connections from neural population A to neural population B . Δt_{AB} are the transmission delays of connections from population A to population B respectively. Here the indexes A and B used to indicate different neural populations can be: S for STN, G for GPe, C for cortex and X for striatum. For clarity, we refer to this set of equations as the ‘original model’, to distinguish it from the two simplified models we consider in the Results section.

B. Determining parameter values

For many of the parameters of the model we were able to determine their values on the basis of published experimental studies (see table I). We used the results of experimental studies from monkeys, unless stated otherwise. However there is a type of parameter that cannot be directly estimated from experimental studies, i.e. the synaptic weights of the network. The values of these synaptic weights were estimated by fitting the behaviour of the model to a wide range of experimental recordings of neuronal activity.

With the advance of Parkinson’s disease dopamine is depleted in the basal ganglia, and experimental evidence suggests that this depletion has an effect the synaptic weights of the STN-GPe network. In the terms of our model, this

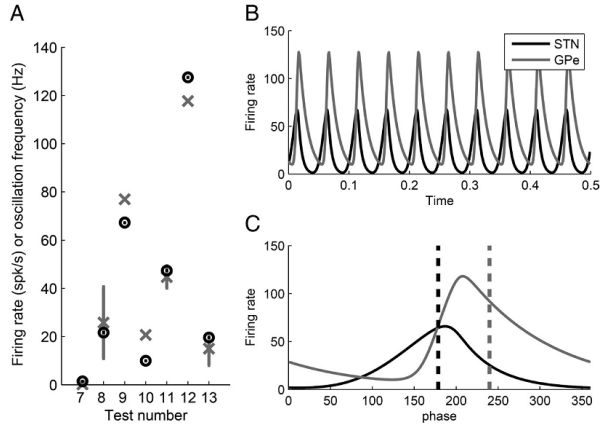


Figure 3. Comparison of model behaviour with experimental data obtained from monkey models of Parkinson’s disease. A: Comparison of the experimental measurements with the corresponding values observed in the computational model. The numbers under the x-axis indicate different experimental recordings used. For measurements 7 to 12, vertical axis indicates firing rate in spk/s, while for measurement 13 it indicates oscillation frequency in Hz. Black circles correspond to the equivalent values using model simulations, while grey crosses show the mean experimental values. In measurement 8 and 11 grey vertical lines indicate standard deviation, while in measurement 13 it indicates the frequency range observed in studies by [46], [47]. The numbers under the x-axis correspond to: (7) STN oscillations minimum firing rate; (8) STN mean firing rate; (9) STN oscillations maximum firing rate; (10) GPe oscillations minimum firing rate; (11) GPe mean firing rate; (12) GPe oscillations maximum firing rate; (13) STN and GPe oscillations frequency. B: Firing rate of the STN and GPe generated by the model for the same parameter values as figure ‘A’. C: A single cycle of oscillation from panel b. The horizontal axis shows the phase of the oscillation, where phase 0° corresponds to the lowest GPe firing rate. The vertical dashed line shows the mean value of phase of each nuclei, which was calculated using the standard equation for the mean of a circular quantity (in this case, the phase).

would be the main alteration to our parameters, and therefore we decided to fit two sets of experimental recordings separately - one obtained from healthy animals (see figure 2) and other obtained from parkinsonian animals (MPTP monkeys, see figure 3). In accordance with experimental evidence, the synaptic weights that we obtained when fitting the healthy data were smaller than the ones obtained when fitting parkinsonian data.

III. RESULTS

A. The mathematical model generates beta oscillations in the parkinsonian state

When the model was simulated with parameter values corresponding to a healthy state, the firing rate of STN and GPe populations converged to a stable state and the model did not produce oscillations (figure 4A and D). However, when the synaptic weights were linearly increased towards the values obtained when fitting parkinsonian data, prominent oscillations in the beta band become apparent (see figure 4B,C,E and F). A bifurcation analysis of this phenomena indicates that the system goes through a Hopf bifurcation as the synaptic weights are increased (see figure 4G). This bifurcation accurately generates the same range of oscillations as observed in Parkinson’s disease (see figure 4H), which are termed beta oscillations in the literature of the disease.

B. Conditions for the onset of oscillations

The study summarised in the previous subsection shows that the system goes through a Hopf bifurcation when the weights are linearly increased from the healthy to the parkinsonian parameters. However they do not confirm if this same bifurcation is the one affecting the system in all cases - i.e. if the system advances towards the parkinsonian state following another nonlinear path through the parametric space. To investigate how general the Hopf bifurcation is (i.e. the extent of the Hopf bifurcation surface in the parametric space), we derive analytically the conditions that generate such oscillations in the parkinsonian state.

To investigate the origin of oscillations analytically, we consider two consecutive reductions of the original model. The first reduction consists on approximating the sigmoidal activation function in the original model by a linear function. We think that this linearisation plus a lower boundary imposed on the activity of the STN and GPe (the variables STN and GP , which represent firing rates, cannot acquire negative values) correctly approximates the behaviour of the original system in the activity range of STN and GP . The second simplification of the original model is the assumption that both time constants and all transmission delays are equal, as the literature reports that they adopt similar values. To distinguish between models, we will refer to the first model as the *original model*, the second one and the *delayed linear model* and the last one as the *nondelayed linear model*. The equations of the delayed linear model are:

$$\begin{cases} \tau \dot{STN}(t) = -STN(t) - w_{GS}GP(t - \Delta t) + w_{CS}Ctx \\ \tau \dot{GP}(t) = -GP(t) + \\ w_{SG}STN(t - \Delta t) - w_{GG}GP(t - \Delta t) - w_{XG}Str \end{cases} \quad (2)$$

while the equations of the nondelayed linear are:

$$\begin{cases} \tau \dot{STN}(t) = -STN(t) \\ -w_{GS} \left(GP(t) - \Delta t \cdot \dot{GP}(t) \right) + w_{CS}Ctx \\ \tau \dot{GP}(t) = -GP(t) - w_{XG}Str + \\ w_{SG} \left(STN(t) - \Delta t \cdot \dot{STN}(t) \right) - w_{GG} \left(GP(t) - \Delta t \cdot \dot{GP}(t) \right) \end{cases} \quad (3)$$

If the nondelayed linear model is analysed, it can be detected that under three conditions the system will generate oscillations. First, the steady state of this STN-GPe system has to be unstable. Second, the trajectories starting from the neighborhood of the steady state should form clockwise spirals, something that can be detected formally if the curl of the (STN, GP) flow is calculated. The third condition required for oscillations is that a closed loop trajectory is formed between the intersection of the boundaries and one of the spiral paths. The mathematical form of each one of these three conditions can be derived analytically (see [48]) obtaining:

$$w_{SG}w_{GS} \frac{\Delta t}{\tau} > 1 + w_{GG} \left(1 - \frac{\Delta t}{\tau} \right) / 2 \quad (4)$$

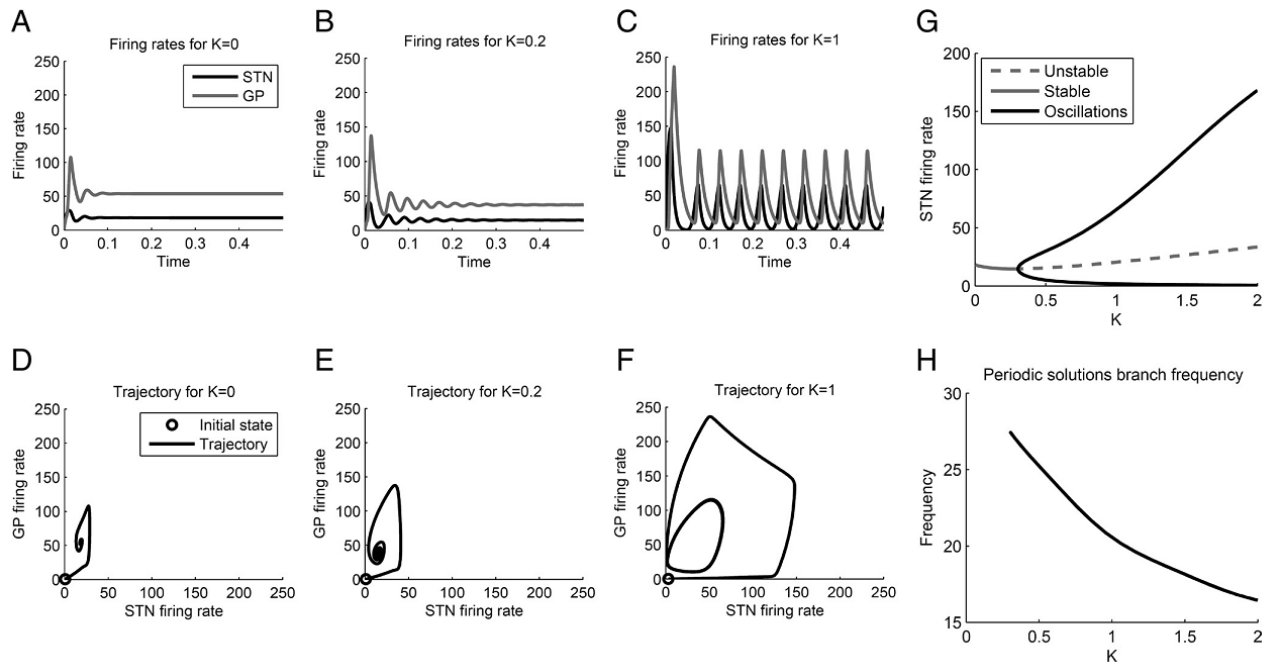


Figure 4. Simulations of the original model. A, B, C: Firing rate as a function of time for different values of K . D, E, F: Phase portraits of the system showing the same firing rates as in A, B and C. G: Range of firing rates of STN as a function of parameter K . A stable steady state is shown with a solid grey line. The unstable steady state is shown with a dashed grey line. The maximum and minimum values in a cycle of oscillations are shown in black. H: Frequency of the oscillations for different values of K . Note that the model predicts a decrease in frequency of oscillation as the weights increase.

for the first condition,

$$w_{SG}w_{GS} > w_{GG}^2/4 \quad (5)$$

for the second condition, and

$$w_{SG}w_{CS}C\tau > w_{XG}Str \quad (6)$$

for the third condition.

C. Comparison of analytical results with numerical simulations

The three conditions derived in the previous subsection form a hyperdimensional surface in the parametric space of the synaptic weights, which corresponds with a Hopf bifurcation surface in the nondelayed linear model. To study the validity of this bifurcation surface in the *original* and *delayed* models, we simulated these systematically in all nodes of a mesh in parameter space. For each node, its main frequency and power is represented in figure 5, where the extent of the oscillatory area can be compared with the analytical bifurcation surface.

It can be observed that the analytical surface matches closely with the surface calculated numerically in the delayed linear model (see figure 5A). In the original model the surface follows the same shape (dashed line in figure 5B), while the position is not as accurate as in the previous model due to the nonlinear shape of the sigmoidal function. To further approximate the original surface, a different linearisation point can be used when linearising the sigmoidal function. If this point is selected around the average value that STN

and GP adopt during the parkinsonian oscillations, a closer match can be obtained (solid line in the figure). It can also be observed that the transmission delays (Δt) and time constants (τ) of the model define the frequency of the parkinsonian oscillations, but not so the synaptic weights. If the Δt and τ are set to the experimentally recorded values, beta oscillations will be obtained.

IV. ACKNOWLEDGMENTS

Dr Alejo J Nevado-Holgado was funded by Caja Madrid Foundation, Madrid, Spain, at the time of the study. We thank Prof Kevin Gurney and Dr Peter Magill for proof-reading the original detailed manuscript of the study[48], on which this conference paper is mostly based, before submitting to Journal of Neuroscience.

REFERENCES

- [1] Albin, R. L., Young, A. B., and Penney, J. B. *Trends Neurosci* **12**(10), 366–375 Oct (1989).
- [2] Bezard, E., Dovero, S., Prunier, C., Ravenscroft, P., Chalon, S., Guilloteau, D., Crossman, A. R., Bioulac, B., Brotchie, J. M., and Gross, C. E. *J Neurosci* **21**(17), 6853–6861 Sep (2001).
- [3] DeLong, M. R. and Wichmann, T. *Arch Neurol* **64**(1), 20–24 Jan (2007).
- [4] Galati, S., D’angelo, V., Scarnati, E., Stanzione, P., Martorana, A., Procopio, T., Sancesario, G., and Stefani, A. *Synapse* **62**(6), 409–420 Jun (2008).
- [5] Greenamyre, J. T. *J Neural Transm Gen Sect* **91**(2-3), 255–269 (1993).
- [6] Cragg, S. J., Baufreton, J., Xue, Y., Bolam, J. P., and Bevan, M. D. *Eur J Neurosci* **20**(7), 1788–1802 Oct (2004).
- [7] Obeso, J. A., Rodríguez-Oroz, M. C., Rodríguez, M., Lanciego, J. L., Artieda, J., Gonzalo, N., and Olanow, C. W. *Trends Neurosci* **23**(10 Suppl), S8–19 Oct (2000).

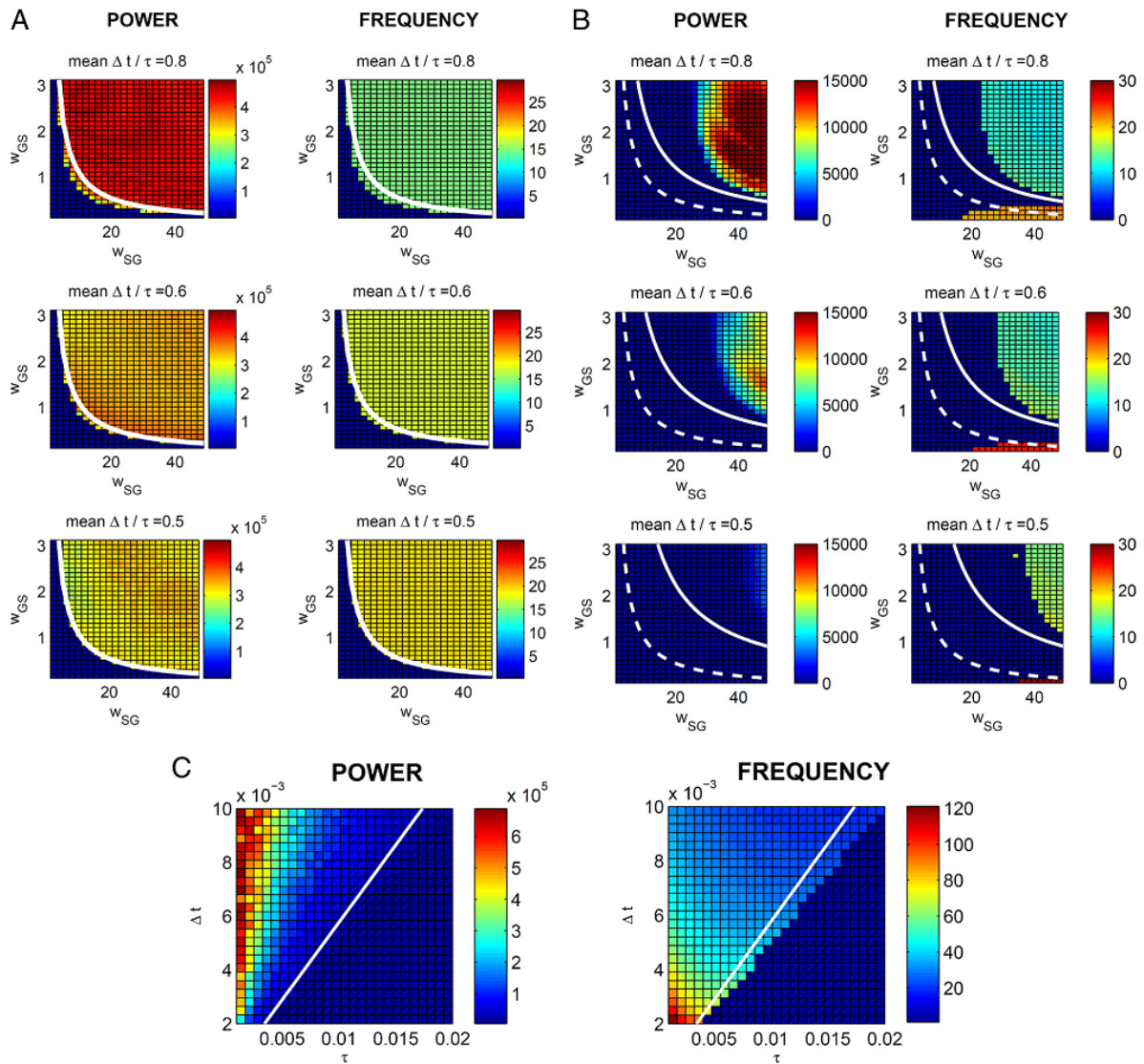


Figure 5. Comparison of analytic and numerical results. Comparison of conditions for the occurrence of oscillations with the simulations of the *delayed linear* (A) and *original models* (B and C) for different values of parameters. In each panel, the left column shows the power spectral density of dominant oscillations, and the right column shows its frequency (Hz). In the simulations of the delayed linear model in panel (A) all parameter were kept as for simulations of the healthy state, except for w_{SG} , w_{GS} , τ , Δt . The values of w_{SG} and w_{GS} are shown on the axes, $\tau = 10ms$ i.e. the average of τ_S and τ_G in the healthy state, and Δt is equal to 15.3ms, 12.8ms and 10.3ms in each of the rows, respectively. Analogously, in the simulations of the original model in panel (B), the values of w_{SG} and w_{GS} are shown on the axes, τ_S and τ_G are set to the values in the healthy state, and Δt_{SG} , Δt_{GS} and Δt_{GG} are increased from the values in the healthy state by 10ms, 7.5ms and 5ms in each of the rows, respectively. In the simulations of the original model in panel (C), all parameters were kept as for simulations of the healthy state, except for τ_S , τ_G , Δt_{SG} , Δt_{GS} and Δt_{GG} that were set as shown on the axes.

- [8] Sohn, Y. H. and Hallett, M. *Scientific Basis for the Treatment of Parkinson's Disease*, chapter 2 - Basal ganglia, motor control and parkinsonism, 33–51. Taylor & Francis (2005).
- [9] Utter, A. A. and Basso, M. A. *Neurosci Biobehav Rev* **32**(3), 333–342 (2008).
- [10] Vingerhoets, F. J., Schulzer, M., Calne, D. B., and Snow, B. J. *Ann Neurol* **41**(1), 58–64 Jan (1997).
- [11] Bogacz, R. and Gurney, K. *Neural Comput* **19**, 442–477 (2007).
- [12] Haber, S. N. *Scientific Basis for the Treatment of Parkinson's Disease*, chapter 1- The basal ganglia, 1–31. Taylor & Francis (2005).
- [13] Parent, A. and Hazrati, L. N. *Brain Res Brain Res Rev* **20**(1), 91–127 Jan (1995).
- [14] Parent, A. and Hazrati, L. N. *Brain Res Brain Res Rev* **20**(1), 128–154 Jan (1995).
- [15] Redgrave, P., Prescott, T. J., and Gurney, K. *Neuroscience* **89**(4), 1009–1023 (1999).
- [16] Boraud, T., Brown, P., Goldberg, J. A., Graybiel, A. M., and Magill, P. J. *The Basal Ganglia VIII*, volume Volume 56 of *Advances in Behavioral Biology*, chapter Oscillations in the Basal Ganglia: The good, the bad, and the unexpected, 1–24. (2005).
- [17] Brown, P. *Movement Disorders Volume 18 Issue 4*, 357 – 363 (2002).
- [18] Gale, J. T., Amirmovin, R., Williams, Z. M., Flaherty, A. W., and Eskandar, E. N. *Neurosci Biobehav Rev* **32**(3), 378–387 (2008).
- [19] Kopell, B. H. and Greenberg, B. D. *Neurosci Biobehav Rev* **32**(3), 408–422 (2008).
- [20] Dauer, W. and Przedborski, S. *Neuron* **39**(6), 889–909 Sep (2003).
- [21] Hammond, C., Bergman, H., and Brown, P. *Trends Neurosci* **30**(7), 357–364 Jul (2007).
- [22] Smith, Y., Bevan, M. D., Shink, E., and Bolam, J. P. *Neuroscience* **86**(2), 353–387 Sep (1998).

- [23] Bevan, M. D., Magill, P. J., Terman, D., Bolam, J. P., and Wilson, C. J. *Trends Neurosci* **25**(10), 525–531 Oct (2002).
- [24] Hutchison, W. D., Lozano, A. M., Tasker, R. R., Lang, A. E., and Dostrovsky, J. O. *Exp Brain Res* **113**(3), 557–563 Mar (1997).
- [25] Lang, A. E. and Zadikoff, C. *Handbook of essential tremor and other tremor disorders*, chapter 13 - Parkinsonian Tremor, 195–220. Taylor & Francis (2005).
- [26] Levy, R., Hutchison, W. D., Lozano, A. M., and Dostrovsky, J. O. *J Neurosci* **20**(20), 7766–7775 Oct (2000).
- [27] Levy, R., Ashby, P., Hutchison, W. D., Lang, A. E., Lozano, A. M., and Dostrovsky, J. O. *Brain* **125**(Pt 6), 1196–1209 Jun (2002).
- [28] Raethjen, J., Lindemann, M., Schmaljohann, H., Wenzelburger, R., Pfister, G., and Deuschl, G. *Mov Disord* **15**(1), 84–94 Jan (2000).
- [29] Kita, H., Tachibana, Y., Nambu, A., and Chiken, S. *J Neurosci* **25**(38), 8611–8619 Sep (2005).
- [30] Sato, F., Parent, M., Levesque, M., and Parent, A. *J Comp Neurol* **424**, 142 – 152 (2000).
- [31] Sato, F., Lavallée, P., Lévesque, M., and Parent, A. *J Comp Neurol* **417**, 17 – 31 (2000).
- [32] Kita, H. *Prog Brain Res* **160**, 111–133 (2007).
- [33] Dayan, P. and Abbott, L. F. *Theoretical Neuroscience*. MIT press, (2001).
- [34] Vogels, T. P., Rajan, K., and Abbott, L. F. *Annu Rev Neurosci* **28**, 357–376 (2005).
- [35] Courtemanche, R., Fujii, N., and Graybiel, A. M. *J Neurosci* **23**(37), 11741–11752 Dec (2003).
- [36] Sharott, A., Magill, P., Harnack, D., Kupsch, A., Meissner, W., and Brown, P. *European Journal of Neuroscience* **21**, 1413–1421 (2005).
- [37] Fujimoto, K. and Kita, H. *Brain Res* **609**(1-2), 185–192 Apr (1993).
- [38] Kita, H., Chang, H. T., and Kitai, S. T. *Brain Res* **264**(2), 255–265 Apr (1983).
- [39] Nakanishi, H., Kita, H., and Kitai, S. T. *Brain Res* **437**(1), 35–44 Dec (1987).
- [40] Paz, J. T., Deniau, J.-M., and Charpier, S. *J Neurosci* **25**(8), 2092–2101 Feb (2005).
- [41] Kita, H. and Kitai, S. T. *Brain Res* **564**(2), 296–305 Nov (1991).
- [42] Lebedev, M. A. and Wise, S. P. *Exp Brain Res* **130**(2), 195–215 Jan (2000).
- [43] Schultz, W. and Romo, R. *Exp Brain Res* **71**(2), 431–436 (1988).
- [44] Hallworth, N. E., Wilson, C. J., and Bevan, M. D. *J Neurosci* **23**(20), 7525–7542 Aug (2003).
- [45] Kita, H., Nambu, A., Kaneda, K., Tachibana, Y., and Takada, M. *J Neurophysiol* **92**(5), 3069–3084 Nov (2004).
- [46] Bergman, H., Wichmann, T., Karmon, B., and DeLong, M. R. *J Neurophysiol* **72**(2), 507–520 Aug (1994).
- [47] Raz, A., Vaadia, E., and Bergman, H. *J Neurosci* **20**(22), 8559–8571 Nov (2000).
- [48] Holgado, A. J. N., Terry, J. R., and Bogacz, R. *J Neurosci* **30**(37), 12340–12352 Sep (2010).